# Automatic generation of boundary conditions using Demons non-rigid image registration for use in 3D modality-independent elastography

Thomas S. Pheiffer[a], Jao J. Ou[a], Michael I. Miga[a,b,c]

[a]Vanderbilt University, Department of Biomedical Engineering, Nashville, TN 37235
[b]Vanderbilt University Medical Center, Department of Radiology and Radiological Sciences, Vanderbilt University Medical Center, Nashville, TN 37235
[c]Vanderbilt University Institute for Imaging Science, Vanderbilt University Medical Center, Nashville, TN 37235

## ABSTRACT

Modality-independent elastography (MIE) is a method of elastography that reconstructs the elastic properties of tissue using images acquired under different loading conditions and a biomechanical model. Boundary conditions are a critical input to the algorithm, and are often determined by time-consuming point correspondence methods requiring manual user input. Unfortunately, generation of accurate boundary conditions for the biomechanical model is often difficult due to the challenge of accurately matching points between the source and target surfaces and consequently necessitates the use of large numbers of fiducial markers. This study presents a novel method of automatically generating boundary conditions by non-rigidly registering two image sets with a Demons diffusion-based registration algorithm. The use of this method was successfully performed *in silico* using magnetic resonance and X-ray computed tomography image data with known boundary conditions. These preliminary results have produced boundary conditions with accuracy of up to 80% compared to the known conditions. Finally, these boundary conditions were utilized within a 3D MIE reconstruction to determine an elasticity contrast ratio between tumor and normal tissue. Preliminary results show a reasonable characterization of the material properties on this first attempt and a significant improvement in the automation level and viability of the method.

**KEYWORDS:** elastography, boundary conditions, non-rigid registration, Demons, breast cancer, FEM

## 1. INTRODUCTION

Breast cancer is second only to lung cancer in cancer-induced mortality among women. For 2009, the American Cancer Society projected over 194,000 new diagnoses of invasive breast cancer, 62,000 cases of *in situ* disease, and an estimated 40,000 deaths from breast cancer in that year. Additional statistics continue to highlight the importance of early initiation of therapeutic measures, as five-year relative survival rates for women diagnosed with advanced or metastatic cancer are only approximately 27%, but as high as 98% for early localized disease[1]. Noninvasive and small-diameter tumors are more readily treated and as such, tightly correlated to treatment success and long-term survival[2, 3]. Early detection is therefore both an inherently desirable goal and one which presents demands for more sensitive detection techniques.

Detection of breast cancer lesions has traditionally been accomplished by examination via palpation and screening imaging by X-ray mammography. Palpation is limited by its subjective nature and a short range of detection into the tissue. Mammography, while the current undisputed clinical standard, has had some questionable reliability when used in isolation[4] and can clearly benefit from additional diagnostic techniques. For example, the exploitation of a contrast mechanism based on elastic properties may have considerable potential as a means for characterizing disease states with changes in tissue composition from varied expression of collagen and increased fibroblast activity[5, 6]. Elastography is one such methodology that utilizes a combination of image processing and physical deformation of tissue to create a representation of the mechanical properties of structures inside organs such as the breast[7, 8]. The application of

elastography in breast cancer imaging would be to differentiate and identify pathological changes in tissue architecture resulting in regional differences in mechanical properties, i.e. stiffness. A relatively new method within the field known as 'modality-independent elastography' (MIE) has recently shown potential for supplementing other imaging modalities such as magnetic resonance (MR) and X-ray computed tomography (CT) for detection of solid tumors in soft tissue. MIE involves imaging a tissue of interest before and after compression, and then applying a finite element (FE) soft-tissue model within a nonlinear optimization framework in order to determine the elastic properties of the tissue.

A requirement of the MIE method is that appropriate boundary conditions be designated for use in the biomechanical model. Conventionally, point correspondence methods facilitated by attached fiducials and assisted by thin-plate spline interpolation have been used to create the boundary conditions that nonrigidly map from the undeformed breast surface to the deformed breast surface. A rather tedious task is necessitated in applying and subsequently localizing numerous surface markers within the image space, creating a thin-plate spline mapping, determining point correspondence, and finally calculating a set of Dirichlet boundary conditions. Initial attempts to reduce the complexity and level of user interaction have focused on the use of energy minimization techniques[9], but the ideal method would be fully automated and require no fiducials. This study presents the latest work in creating a method for automatically generating boundary conditions through the use of a non-rigid image registration algorithm. We present a Demons diffusion non-rigid registration technique used to perform image matching of two sets of pre- and post-deformation images and tested against a controlled *in silico* simulation with known boundary conditions. The generated boundary conditions were also used to perform an MIE elasticity reconstruction to evaluate its effectiveness in determining the elasticity contrast of a previously characterized system.

## 2. METHODS

### 2.1 MIE Workflow

As described in previous work[10], the MIE algorithm is comprised of three major components: 1) a biomechanical FE model of soft-tissue deformation based on material properties, 2) a similarity metric with which to compare images, and 3) an optimization routine to update the material properties in the model.

The process of generating an elasticity reconstruction begins with the acquisition of pre- and post-deformation images of the breast. The breast is then segmented and its surface geometry can be extracted using the marching cubes algorithm and a finite element mesh is created from the surface information. The mesh is partitioned into a desired number of 'regions' to which elasticity properties are assigned, which defines the resolution of the reconstruction. It is then necessary to designate the loading/boundary conditions for the FE model. The ability of the biomechanical model to accurately deform the mesh of the breast tissue is dependent on these boundary conditions. The boundary condition step in the MIE workflow is highlighted in Figure 1.

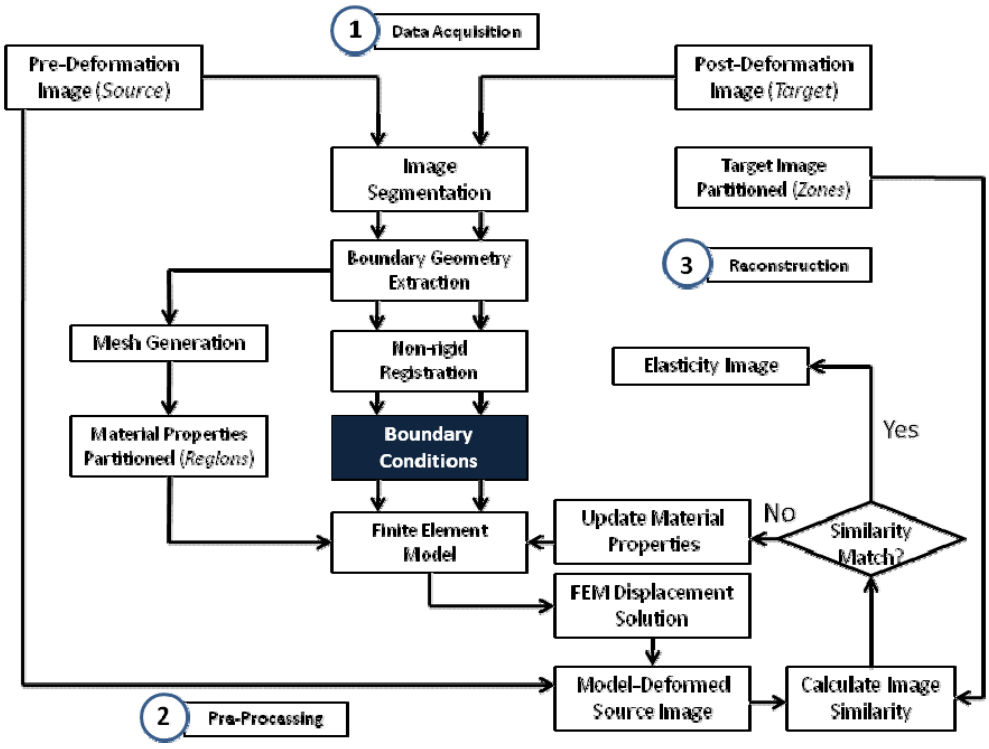


Figure 1. Overview of the MIE protocol. The boundary condition task is seen to be in a central location and has a critical impact on the final reconstruction.

Once boundary conditions have been designated, the model is run and the FEM displacement solution for all the nodes in the mesh is obtained. The displacements are then used to warp the original pre-deformation image, which is then compared with the known post-deformation image to generate an image similarity measurement. A non-linear optimization framework is used to update the material properties of the mesh until the similarity metric is within tolerance, at which point the elasticity reconstruction image is produced.

### 2.2 Automatic Generation of Boundary Conditions

The Demons registration algorithm utilizes a diffusion model in which the object boundaries in one image are characterized as semi-permeable membranes, and the other image is allowed to diffuse through these membranes[11]. Following the formulation of Ibanez, *et al.*[12],

$$\mathbf{D}(\mathbf{X}) \cdot \nabla f(\mathbf{X}) = -(\mathbf{m}(\mathbf{X}) - \mathbf{f}(\mathbf{X})) \tag{1}$$

where $\mathbf{f}(\mathbf{X})$ is the fixed target image, $\mathbf{m}(\mathbf{X})$ is the source image being deformed for the registration, and $\mathbf{D}(\mathbf{X})$ is the displacement field mapping the source to the target image through an instantaneous optical flow. This can be reformulated in an algorithmic iterative form as follows:

$$\mathbf{D}^{N}(\mathbf{X}) = \mathbf{D}^{N-1}(\mathbf{X}) - \frac{\left(\mathbf{m}\left(\mathbf{X} + \mathbf{D}^{N-1}(\mathbf{X})\right) - \mathbf{f}(\mathbf{X})\right)\nabla \mathbf{f}(\mathbf{X})}{\|\nabla \mathbf{f}\|^{2} + \left(\mathbf{m}\left(\mathbf{X} + \mathbf{D}^{N-1}(\mathbf{X})\right) - \mathbf{f}(\mathbf{X})\right)^{2}} \tag{2}$$

The displacement field obtained from Equation 2 is smoothed with a Gaussian filter between each iteration in order to enforce elastic-like behavior. This aspect of the algorithm's implementation made it appropriate for modeling the boundary conditions of a system being deformed within the confines of an elastic model.

The registration produces displacements at the centroid of every voxel. The displacement vectors are then interpolated onto the nodal coordinates of the finite element mesh using a cubic 3D interpolation. The displacements which are assigned to boundary nodes are thus designated as the boundary conditions for the elastic model.

For the two data sets, each source image volume was non-rigidly registered to a corresponding deformed image volume using an Insight Toolkit (ITK)-based Demons diffusion-based image registration algorithm via MATLAB (Mathworks, Natick, MA). Both the CT set and the MR set were run through the registration for 3,500 iterations with a Gaussian smoothing kernel standard deviation of 1.5. The resulting boundary displacements were then compared to the known boundary displacements used to originally deform the image sets as described further below.

**2.3 Image Acquisition, Deformation and Mesh Generation**

Two image sets (CT and MR) of normal tumor-free human breast were obtained from the UC-Davis Department of Radiology and the Vanderbilt University Institute of Imaging Science, respectively, for use in this work. These images are referred to as *source* images for the remainder of this document. The surface of the breast was segmented from the surrounding structures using Analyze 8.1 (Mayo Clinic, Rochester, MN) and was used to create a three dimensional finite element mesh using a tetrahedral mesh generation algorithm[13]. For both the CT set and the MR set, a 2-cm spherical tumor was synthetically implanted in the center of the respective mesh and assigned an elasticity value six times higher than the surrounding material. This contrast ratio of 6.00:1 was thus considered to be the goal for reconstruction in both cases. Each finite element mesh was then deformed by applying a depression on one side of the breast. The displacements predicted by the model were then used to deform the CT and MR images. Figures 2a and 2b show an axial slice from the undeformed (left) and deformed (right) CT image volume, respectively. Figures 2c and 2d show an undeformed (left) and deformed (right) slice from the MR image volume, respectively.

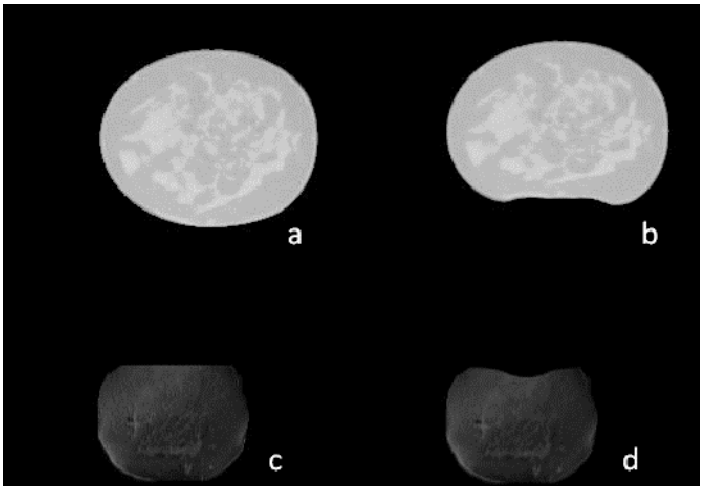


Figure 2. Representative slices from the two data sets used for the simulations. Slice (a) shows the CT image in its undeformed state, and (b) shows the CT image in its deformed state. Slice (c) shows the MR image in its undeformed state, and (d) is the MR image in its deformed state.

The depression as seen in Figure 2 was used to create gold standard boundary conditions for testing the accuracy of the demons registration algorithm and the deformed target images were used to test the accuracy and fidelity of the 3D MIE

reconstructions. The MIE reconstructions have been described below and the accuracy results have been presented in the following section.

### 2.4 3D MIE Reconstruction Using Boundary Conditions Generated Automatically by the Demons Algorithm

The 3D MIE reconstruction algorithm presented in previous work[14] was used to localize the lesion by utilizing the boundary conditions generated by the Demons algorithm. *A priori* spatial knowledge of the location of the cancerous inclusion was used to constrain the algorithm to two regions of material properties: 1) the tumor, and 2) the surrounding normal tissue. Both regions were set to have the same initial material property values. The similarity of the CT set was sampled regionally using 136 zones (the MIE method samples similarity to assist in reconstruction), while the similarity of the MR set was sampled using 110 zones. The algorithm was allowed to run until convergence, which was defined to be a minimum relative change in the image similarity metric. The Demons-derived boundary conditions were utilized for the MIE reconstruction and tumor-to-normal-tissue stiffness ratios were compared to their known counterparts of 6:1 for tumor-to-normal tissue. The results have been presented in Section 3.

## 3. RESULTS

### 3.1 CT Simulation

Figure 3 displays the results of the automatic boundary condition method applied to the CT data set as described above. Figure 3a shows the mesh after it has been deformed by the originally specified boundary conditions. The lighter areas of the mesh represent greater displacements from the original undeformed mesh. The light rectangular area on the right side of the mesh corresponds to the artificial depression. Figure 3b shows the mesh after it has been deformed instead by the Demons registration boundary conditions.

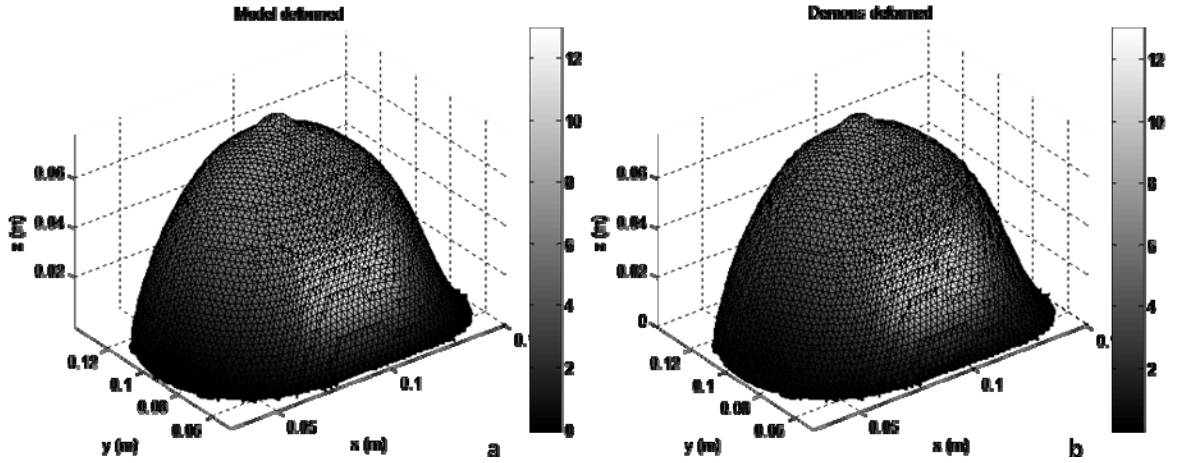


Figure 3. Deformed mesh using the model displacements (a) and using the Demons-derived displacements (b). The colorbar indicates the magnitude of the surface displacements in millimeters.

The maximum displacement in the known boundary conditions occurred in the depression and was approximately 13 mm in magnitude. The Demons registration was able to reproduce this displacement very well as can be seen in a direct visual comparison of Figures 3a and 3b.

Figure 4 shows the distribution of error between the original known boundary conditions and the automatically-generated boundary conditions from the non-rigid registration. This error is defined as the difference in displacement magnitude at each node between the two sets of conditions. The lighter areas of the mesh correspond to areas that experienced greater error when compared to the known boundary conditions. As seen in the figure, the largest errors

were spread across the region of high curvature around the tip of the breast and in the dip of the artificial depression. Averaging over all the nodes on the boundary, a mean error of 0.6 mm ±0.3 mm was obtained, which represents an average difference of about 17%. The minimum error on the boundary was 0.02 mm, while the maximum error was about 1.5 mm.

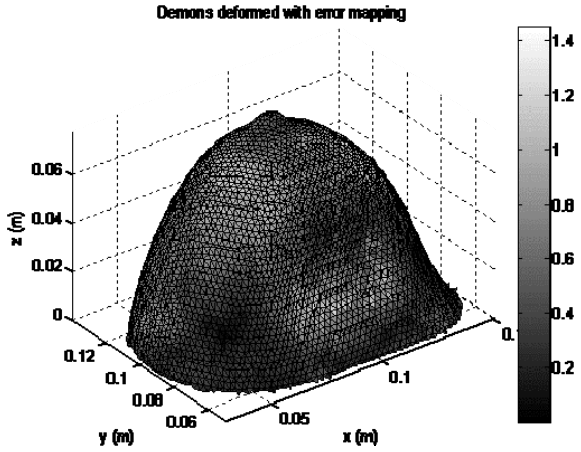


Figure 4. Visualization of error between the Demons-derived boundary conditions and the known boundary conditions. The colorbar indicates the magnitude of the surface displacements in millimeters.

Figure 5a shows an axial slice of the breast volume with the tumor in the center (white region shown in the figure). This image volume was used as the target image volume for the MIE algorithm and the tumor-to-normal tissue elasticity ratio was set at 6.00:1. Figure 5b shows the mesh with the tumor as reconstructed by the MIE algorithm using the automatic boundary conditions. The MIE algorithm predicted a tumor-to-normal tissue elasticity ratio of 8.65:1.

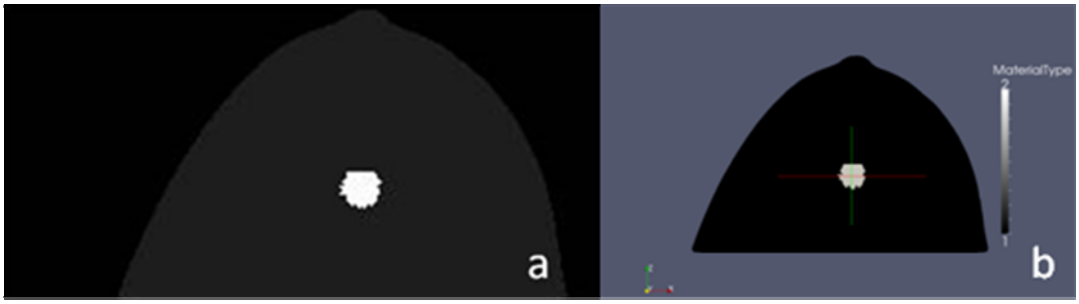


Figure 5. (a) True elasticity image set showing the tumor in the center (white) used to create simulation (b) MIE reconstruction of the domain. Material type 1 (black surrounding region) represents normal/benign tissue. Material Type 2 (white central tissue) represents the tumor. The tumor-to-normal tissue elasticity constant ratio found by MIE was 8.65:1.

### 3.2 MR Simulation

Figure 6 displays the results of the automatic boundary condition method described, as applied to the MR data set. Figure 6a is the mesh after it has been deformed by the originally specified boundary conditions. As in the CT simulation, the lighter areas on the mesh correspond to greater displacements from the original mesh. The lighter area at the top of the mesh is the site of the artificial applied depression. Figure 6b shows the mesh after it has been deformed instead by the Demons registration boundary conditions.

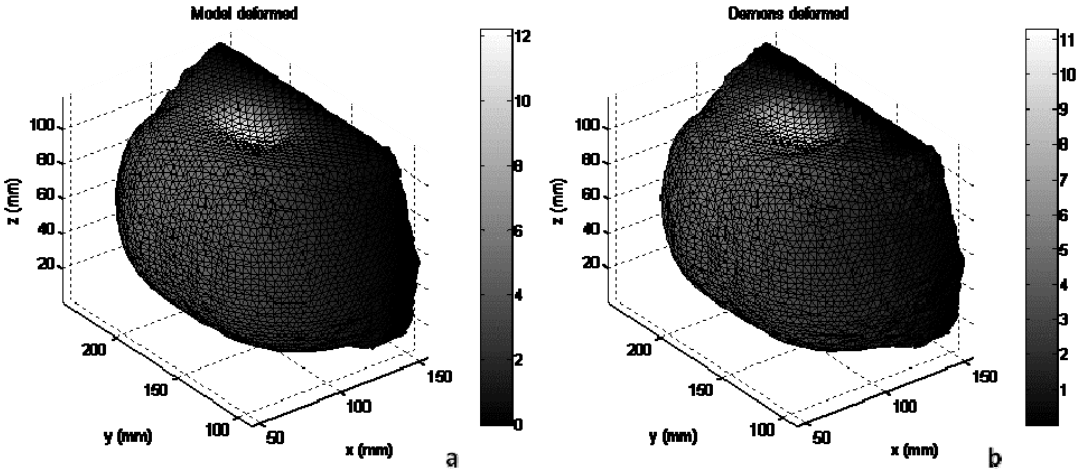


Figure 6. Deformed mesh using the model displacements (a) and using the Demons-derived displacements (b). The colorbar represents the magnitude of the surface displacements in millimeters.

The maximum displacement in the known boundary conditions had a magnitude of about 12 mm and was located in the depression. The Demons registration reproduced this displacement to within about 1 mm.

Figure 7 shows the distribution of error between the original known boundary conditions and the automatically-generated boundary conditions from the non-rigid registration. The error is defined in Section 3.1. The lighter areas of the mesh correspond to areas that experienced greater error when compared to the known boundary conditions. As seen in the figure, the largest errors were spread across the region of high curvature, as in the dip of the artificial depression. Averaging over all the nodes in the mesh, a mean error of 0.5 mm ± 0.3 mm was obtained, which represents a mean error of about 23%. The maximum error that occurred on the boundary was about 1.9 mm, while the minimum error was about 0.01 mm.

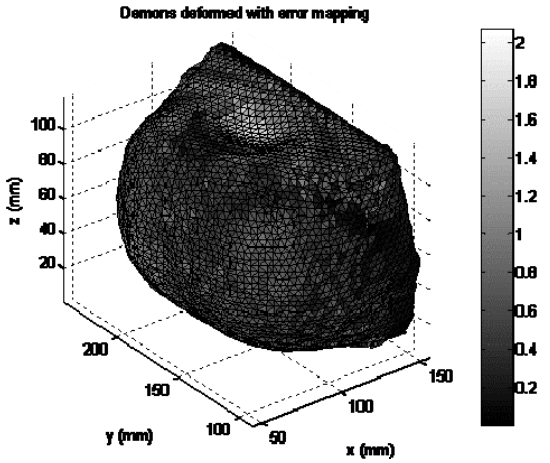


Figure 7. Visualization of error between the Demons-derived boundary conditions and the known boundary conditions. The colorbar represents the magnitude of the surface displacements in millimeters.

Figure 8a shows an axial slice of the breast volume with the tumor in the center (white region shown in the figure). This image volume was used as the target image volume for the MIE algorithm and the tumor-to-normal tissue elasticity ratio was set at 6.00:1. Figure 8b shows the mesh with the tumor as reconstructed by the MIE algorithm using the automatic boundary conditions. The MIE algorithm predicted a tumor-to-normal tissue elasticity ratio of 5.53:1.

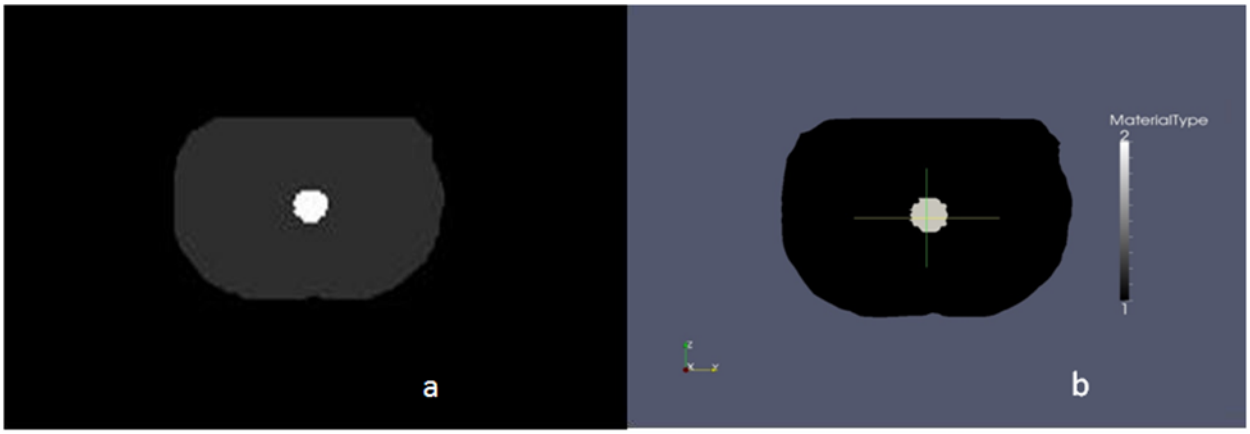


Figure 8. (a) True elasticity image set showing the tumor in the center (white region) used for MIE reconstruction (b) MIE reconstructed mesh. Material type 1 (large surrounding region) represents normal/benign tissue. Material Type 2 (small region in the center) represents the tumor tissue. The tumor-to-normal tissue elasticity constant ratio found by MIE was 5.53 to 1.

## 4. DISCUSSION

In the implementation of the Demons algorithm, no unique difficulties were encountered in its application to the CT or MR image sets, demonstrating that automation in the context of modality independence is possible. The only user interaction required in this framework was the designation of the input parameters for the registration. Ideally, the boundary conditions obtained from the automatic non-rigid registration should equate to the known boundary conditions for the mesh that created the deformed target image. The results above show that the average error between these two sets of boundary conditions at the nodes was approximately the spacing of a voxel for the CT set, and less than half the spacing of a voxel for the MR set. The MR set thus had loading conditions within the working tolerance of the MIE algorithm to boundary condition error[14] in order to create a reasonable reconstruction. Despite the somewhat higher error on the boundary for the CT set, a reasonable reconstruction was obtained. It is likely that this is because the elastic nature of the non-rigid registration constrained the model to realistic deformations. For the application of the Demons registration-based boundary conditions to the CT data set, the elasticity reconstruction with spatial *a priori* knowledge of the tumor successfully converged to a contrast ratio of 8.65:1. Similarly, the MR data resulted in a contrast ratio of 5.53:1. Compared to the known designated material contrast of 6.00:1, there is clearly a discrepancy in these reconstruction behaviors that needs to be investigated. The difference, particularly between the different modalities of input data, is likely due to a combination of factors including mesh geometry and image quality. In addition, the distance of the tumor from the area of greatest displacement likely affects the accuracy of the reconstruction, since the displacements of nodes are expected to decrease the further they are located away from the depression. These areas all remain avenues of further exploration to fully characterize the behavior of the MIE algorithm.

## 5. CONCLUSIONS

A novel method for automatically generating boundary conditions for a finite-element elastic model from a non-rigid image registration has been presented in this work. The Demons algorithm was able to generate physically realistic boundary conditions with an acceptable level of accuracy when compared against a controlled biomechanical model. These boundary conditions were also used to generate MIE elasticity reconstructions, with encouraging initial results. Additional work to validate the effectiveness of this new method of generating boundary conditions is being planned with additional image volumes as well as real-world testing using phantom experiments and correlation to material testing data and histology.

## ACKNOWLEDGEMENTS

We gratefully acknowledge support from the Vanderbilt University Institute of Imaging Science in providing their implementation of the Demons non-rigid registration algorithm, which benefited from the use of ITK (U.S. National Library of Medicine, www.itk.org). The image data appearing within are the generous donations of John Boone, PhD of the University of California-Davis and Thomas Yankeelov, PhD of the Vanderbilt University Institute of Imaging Science. Additional thanks to Prashanth Dumpuri, PhD of the Vanderbilt University Department of Biomedical Engineering for technical and experimental support

## REFERENCES

[1] ACS, "Cancer Facts & Figures 2009," American Cancer Society, (2009).
[2] Michaelson, J. S., Silverstein, M., Wyatt, J., Weber, G., Moore, R., Halpern, E., Kopans, D. B., and Hughes, K., "Predicting the survival of patients with breast carcinoma using tumor size," Cancer **95,** 713-723 (2002)
[3] Warwick, J., Tabar, L., Vitak, B., and Duffy, S. W., "Time-dependent effects on survival in breast carcinoma: results of 20 years of follow-up from the Swedish Two-County Study," Cancer **100,** 1331-1336 (2004)
[4] Keith, L. G., Oleszczuk, J. J., and Laguens, M., "Are mammography and palpation sufficient for breast cancer screening? A dissenting opinion," J Womens Health Gend Based Med **11,** 17-25 (2002)
[5] Burns-Cox, N., Avery, N. C., Gingell, J. C., and Bailey, A. J., "Changes in collagen metabolism in prostate cancer: a host response that may alter progression," J Urol **166,** 1698-1701 (2001)
[6] Lee, H., Sodek, K. L., Hwang, Q., Brown, T. J., Ringuette, M., and Sodek, J., "Phagocytosis of collagen by fibroblasts and invasive cancer cells is mediated by MT1-MMP," Biochem Soc Trans **35,** 704-706 (2007)
[7] Bilgen, M., "Target detectability in acoustic elastography," Ieee Transactions on Ultrasonics Ferroelectrics and Frequency Control **46,** 1128-1133 (1999)
[8] Doyley, M. M., Meaney, P. M., and Bamber, J. C., "Evaluation of an iterative reconstruction method for quantitative elastography," Phys Med Biol **45,** 1521-1540 (2000)
[9] Ong, R. E., Ou, J. J., and Miga, M. I., "Using Laplace's equation for non-rigid registration of breast surfaces," Medical Imaging 2007: Visualization and Image-Guided Procedures: Proc. of the SPIE, (in press)**,** (2007)
[10] Miga, M. I., Rothney, M. P., and Ou, J. J., "Modality independent elastography (MIE): potential applications in dermoscopy," Med Phys **32,** 1308-1320 (2005)
[11] Thirion, J. P., "Image matching as a diffusion process: an analogy with Maxwell's demons," Med Image Anal **2,** 243-260 (1998)
[12] Ibanez, L., Schroeder, W., Ng, L., and Cates, J., [The ITK Software Guide] Kitware, Inc., (2005).
[13] Sullivan, J. M., Charron, G., and Paulsen, K. D., "A three-dimensional mesh generator for arbitrary multiple material domains," Finite Elements in Analysis and Design **25,** 219-241 (1997)
[14] Ou, J. J., Ong, R. E., Yankeelov, T. E., and Miga, M. I., "Evaluation of 3D modality-independent elastography for breast imaging: a simulation study," Phys Med Biol **53,** 147-163 (2008)